SANS Study of Polymer−Supercritical Fluid Solutions: Transitions from Liquid to Supercritical Fluid Solvent Quality

T. P. DiNoia,[†] C. F. Kirby,[†] J. H. van Zanten,[‡] and M. A. McHugh*[,§]

Department of Chemical Engineering, Johns Hopkins University, Baltimore, Maryland 21218; Chemical Engineering Department, North Carolina State University, Box 7905, Raleigh, North Carolina 27695-7905; and Department of Chemical Engineering, Virginia Commonwealth University, Richmond, Virginia 23284

Received February 8, 2000; Revised Manuscript Received June 21, 2000

ABSTRACT: Phase behavior and small-angle neutron scattering (SANS) measurements are reported for poly(ethylene-*co*-1-butene) (PEB) dissolved in pentane, pentane plus ethane, and supercritical ethane to pressures of 2000 bar and temperatures of 130 and 150 °C. The solution microstructure and solvent quality are probed using the high-concentration isotopic labeling technique at the mixture critical concentration to determine the variation of intra- and intermolecular correlations on approach to the phase boundary with isothermal changes in pressure. The SANS results for the three solutions show that the intramolecular radius of gyration remains close to the unperturbed value over the entire pressure range investigated. However, the intermolecular correlation length changes dramatically as the phase boundary is approached and is approximately 3 times larger in ethane as compared to pentane even at 1000 bar from the phase boundary. The intermolecular correlation length data suggest that ethane is a poorer quality solvent than pentane at conditions close to the phase boundary even though both solvents have similar mass densities.

Introduction

Supercritical fluids (SCF) are being considered as solvents for processing foods, nutraceuticals, and polymeric materials, as reaction media for polymerization processes, as environmentally preferable solvents for solution coatings, powder formation, impregnation, encapsulation, cleaning, crystal growth, and antisolvent precipitation, and as mixing/blending aids for crystalline or viscous materials.[1−10] This broad range of applications can be extended further if a better understanding of the underlying physics and chemistry of SCF−solute behavior is established. A significant impediment to the facile application of SCF solvents for processing polymers is the very poor performance of equations of state used to model polymer−SCF mixture behavior.[11−14] Equations of state are still not able to account quantitatively for the intra- and intersegmental interactions of the many segments of the polymer connected to a single backbone relative to the small number of segments in a solvent molecule. In addition, polymer−SCF solutions are both dense and compressible, which makes it difficult to calculate accurately the density dependence of the intermolecular potential functions. A significant amount of experimental phase behavior information now exists on polymer−SCF mixtures from which a coarse-grained interpretation of the impact of solvent quality and polymer architecture on the phase behavior can be obtained.[14] In the present work, a small-angle neutron scattering (SANS) study of polymer−SCF solution behavior is described to obtain fundamental microstructural information. SANS data are obtained at various distances to the phase boundary for poly(ethylene-*co*-1-butene) (PEB) dissolved in liquid *n*-pentane, a mixture of *n*-pentane plus ethane, and supercritical ethane to characterize how solvent quality changes from the liquid to the supercritical fluid state. These PEB/alkane mixtures are chosen since the components have closely matched intermolecular potential functions which facilitates the interpretation of the experimental data.

Although the properties of dilute polymer solutions are well understood, much less is known about the behavior of a polymer chain in the semidilute concentration regime, near the mixture critical point.[15,16] In addition, much less is known about how pressure influences polymer behavior in both incompressible and compressible solvents. Very recently, Melnichenko and co-workers[17−19] used SANS to investigate the effect of temperature and pressure on the intra- and intermolecular interactions of polystyrene in liquid cyclohexane and in liquid acetone at polymer concentrations near the respective solution critical points, close to the chain overlap concentration. They extended these studies to include poly(dimethylsiloxane) (PDMS) in supercritical CO_2 also near the solution critical point.[20] They demonstrated that the radius of gyration (R_g) of the chain, which is associated with polymer intramolecular interactions, does not deviate from the unperturbed θ-melt value as the mixture critical point is approached with changes in pressure or temperature. However, over the same operating space, intermolecular interactions characterized by the correlation length (ξ), rapidly increase near the mixture critical point and can exceed the magnitude of R_g, indicating the presence of strongly interacting unperturbed coils. The SANS studies performed by Melnichenko and co-workers[17−19] confirm the predictions of Muthukumar[21] and Raos and Allegra[22] that polymer chains remain in the unperturbed state as the solvent quality is adjusted below the θ-condition and throughout the poor solvent regime until the critical boundary is reached.

Other than the PDMS−supercritical CO_2 work,[20] the solvents used by Melnichenko and co-workers are dense

[†] Johns Hopkins University.
[‡] North Carolina State University.
[§] Virginia Commonwealth University.

10.1021/ma000240z CCC: $19.00
Published on Web 07/26/2000

liquids far from their respective, pure component, critical conditions. It is difficult to probe large regions of chemical potential space with changes in pressure and temperature when using an incompressible liquid solvent. Conversely, it is straightforward to adjust solvent quality when using a supercritical fluid since its density is sensitive to modest changes in pressure and temperature.[1] The work presented here addresses the question of whether differences exist on a microscopic level between the quality of a liquid and an SCF solvent that are both from the same chemical family. The inference drawn from available polymer−SCF phase behavior studies is that an SCF solvent is an exceptionally weak solvent relative to a liquid.[14] For example, significant differences are exhibited in the phase behavior of poly(ethylene) (PE) in ethane, propane, and butane at 110 °C, which is greater than the critical temperature of ethane (32.3 °C) and propane (96.7 °C) but less than the critical temperature of butane (152.1 °C).[23−25] The pressures needed to obtain a single phase decrease by ∼1000 bar as the molecular weight of the solvent increases from ethane to propane, and it decreases by another 400 bar going from propane to butane. Dispersion forces dominate the PE segment−segment, PE segment−solvent, and solvent−solvent electrostatic attractive interactions expected for these nonpolar polymer−solvent mixtures. Hence, the decrease in coexistence pressure, or conversely the increase in SCF solvent quality, follows directly from the increase in polarizability with increasing solvent size. However, as just noted for the PE−alkane system, the improvement in SCF solvent quality exhibits a diminishing returns effect with increasing molecular size of the solvent. It is the weak solvent quality of low molecular weight supercritical fluids that make them unique for exploring the response of the solution microstructure with changes in the system temperature, pressure, and density.[17]

Experimental Section

Materials. Ethane (99.0% minmum purity) is obtained from Aldrich Chemical Co. for the phase behavior experiments. High-purity ethane (Scientific Grade, 99.95% minimum purity) is obtained from MG Industries for the SANS studies, pentane (n-C_5H_{12}) (99.7% minimum purity) is obtained from Fisher Chemicals, and deuterated pentane-d_{12} (n-C_5D_{12}) (98.0% minimum purity D, 98%) is obtained from Cambridge Isotopes Laboratories for the phase behavior and SANS studies.

Pamela Wright and Lewis Fetters from Exxon Research and Engineering Co. synthesized the fully protonated and partially deuterated poly(ethylene-*co*-20.2 mol % butene) (*h*-PEB-10 and *d*-PEB-10, respectively) used in this study. The PEB copolymers are produced from anionic polymerization of butadiene with subsequent saturation by hydrogenation or deuteration as described in detail elsewhere.[26−29] The *h*-PEB-10 and *d*-PEB-10 have approximately 10 ethyl branches per 100 carbon atoms and weight-average molecular weights (M_W) of 232 500 and 245 000, respectively, with molecular weight distributions of 1.01.

The fully deuterated poly(ethylene-*co*-3 mol % butene) (*d*-PEB-2) used in this study, obtained from Polymer Sources, Inc., has approximately two ethyl branches per 100 carbon atoms, an M_W of 169 000, and a molecular weight distribution of 1.09. It is produced from catalytic polymerization of deuterated 1,3-butadiene (D, ≥99.8%) and is then fully deuterated in a D_2 atmosphere (D, ≥99.8%) at 400 psi and 60 °C for 24 h.

Phase Behavior Determination. The experimental apparatus shown in Figure 1 is briefly described here since details on the high-pressure apparatus and technique are given elsewhere.[30,31] System pressure is determined to within ±3.5 bar with a digital pressure transducer (Viatran Corporation, model 245) or a Heise Gage (Dresser Industries, model CM-108952). System temperature is measured and maintained to within ±0.5 °C. The solution in the cell is well mixed with a magnetic stir bar driven by a rotating external magnet. Cloud points, reproducible to within ±5 bar, are obtained by decreasing the pressure isothermally until the clear single phase becomes so opaque that the stir bar is no longer visible. The mixture critical point is the temperature, pressure, and polymer concentration where two phases of equal volume are observed at the transition, which is also accompanied by reddish-orange opalescence.

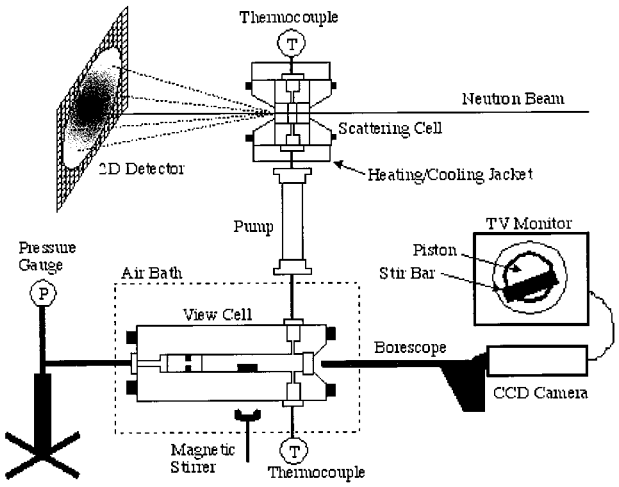

Figure 1. Schematic diagram of the high-pressure equipment used to obtain phase behavior and SANS data.

Small-Angle Neutron Scattering. Figure 1 also shows the high-pressure SANS scattering cell used with the view cell. The polymer solution is well mixed for 1−2 h in the view cell and is then transferred to the scattering cell using a magnetically driven pump. SANS detector counts are monitored during the transfer to ensure that the solution in the scattering cell is a single phase. The scattering cell body, constructed of a high-strength steel alloy (Nitronic 50), is 9.4 cm long and 7.6 cm o.d.[32] The cell is fitted with 1.91 cm o.d. by 1.91 cm thick sapphire windows (±0.003 cm, General Ruby and Sapphire Co., Florida) and, based on an unsupported area of 1.27 cm^2, is rated to 6800 bar with a safety factor of 10. The windows are sealed with elastomeric O-rings in a configuration recommended by Lentz.[33] The path length between the inner surfaces of the windows is adjustable between 0.1 and 0.5 cm using spacers. Each window is retained by an end-cap with a 30° included-angle cone that allows a neutron beam to exit the scattering cell at a maximum angle of 15° relative to the window surface. The solution temperature is measured with a calibrated type-E thermocouple fitted into a cell port and connected to a multimeter (Omega Instruments, Inc., model DP465, accuracy ±0.03%). An aluminum band heater with four resistance heating cartridges and four cooling lines is used to maintain the cell to within ±0.5 °C.

Neutron scattering experiments are performed on the NG-3 30-m SANS spectrometer at the National Institute of Standards and Technology (NIST) located in Gaithersburg, MD. Details of the 30 m SANS instrument at NIST are given elsewhere.[34] A neutron wavelength of 5.0 Å ($\Delta\lambda/\lambda = 0.15$) is used with a sample aperture diameter of 0.64 cm. SANS measurements are performed with five different mixture critical solutions: 2.2 wt % *d*-PEB-2 in ethane, 4.6 wt % *h*-PEB-10 in pentane-d_{12}, 5.2 wt % total polymer (*h*-PEB-10 + *d*-PEB-10) in pentane-d_{12}, 4.5 wt % *h*-PEB-10 in pentane-d_{12} + 23 wt % ethane (polymer-free basis), and 4.5 wt % total polymer (*h*-PEB-10 + *d*-PEB-10) in pentane-d_{12} + 27 wt % ethane (polymer-free basis). An ethane cosolvent concentration of ∼25 wt % is used here since this level of ethane is expected to shift significantly the cloud-point pressure of the PEB−

pentane solution, which is a clear indication that the pentane + ethane mixture behaves as a hybrid solvent with properties between those of liquid pentane and supercritical ethane. The sample-to-detector distance is 6.1 m for the *d*-PEB-2/ethane solution to obtain a q range of $0.01 \leq q \leq 0.14$ Å^{-1} for $q = 4\pi/\lambda \sin(\theta/2)$ where θ is the scattering angle. For the other solutions, sample-to-detector distances of 10.55 and 2.55 m are used to give overlapping q ranges of $0.005 \leq q \leq 0.07$ Å^{-1} and $0.02 \leq q \leq 0.28$ Å^{-1}, respectively.

The measured intensities are corrected for dark-noise background, detector efficiency, scattering from the empty cell with sapphire windows, and sample transmission. Intensities are also corrected for changes in sample path length resulting from window displacement at high pressures that is measured directly for each pressure and temperature with a high-resolution indicator gauge (Starrett Co., model 25-881). The scattered intensities are radially averaged and converted to an absolute differential scattering cross section per unit volume, $d\Sigma/d\Omega$ (cm^{-1}), using cross-section calibration standards of silica and water for the low and high q ranges, respectively.

The incoherent scattering contribution can be estimated using experimentally measured sample transmissions and bound coherent and incoherent cross sections[35−37] with element and isotope neutron scattering cross sections from Sears.[38] However, calculated sample transmissions are always slightly greater than experimentally determined transmissions for each system considered here. Maconnachie argues that the effective cross section is a strong function of temperature and wavelength, which is problematic for the experiments reported here since elevated temperatures of 130 and 150 °C are used to avoid PEB crystallization. Since the temperature dependence of the total cross sections for each semidilute solution is unknown, incoherent background scattering for each sample is determined from the solution scattering at high q values assuming the incoherent scattering is isotropic.

As a check of this assumption, high-q incoherent backgrounds for *d*-PEB-2 in ethane are compared to the incoherent backgrounds obtained from pure ethane scattering at the same pressure and temperature. The absolute differential scattering cross section per unit volume for pure ethane at 130 °C does not depend on q over the entire range investigated, but the scattering intensity does increase with increasing pressure (or density), as expected. The incoherent background is subtracted from the solution scattering after correcting for the concentration of the polymer and pure ethane density to obtain the scattering from the polymer.[39] The estimated incoherent background scattering is similar but not exactly equal to the incoherent background obtained from solution scattering at high q values. This discrepancy may be due to a nonnegligible incoherent scattering contribution from the fully deuterated polymer at semidilute concentrations.[36] Therefore, scattering data are analyzed using incoherent background scattering obtained at q values out to 0.28 Å^{-1} for *h*-PEB-10 and *d*-PEB-10 in pentane-d_{12} and in pentane-d_{12} plus ethane mixtures.

Results

Phase Behavior Measurements. Figure 2 shows that the cloud-point curves for *h*-PEB-10 in pentane and in pentane-d_{12} are at quite modest pressures. Both cloud-point curves, also termed lower critical solution temperature (LCST) curves, intersect the liquid−liquid−vapor (LLV) curve at ∼107 °C, and the slopes of both curves are similar to those reported for binary mixtures of PE in pentane[40−44] and for poly(isobutylene) in alkane solvents.[45] The slope of the LCST curve with deuterated pentane is slightly larger than that with protonated pentane, which means it takes slightly higher pressures to obtain a single phase with the deuterated solvent. Increased cloud-point pressures are expected since replacing hydrogen with deuterium affects the magnitude of the intermolecular pair potential energies (Γ) and the interchange energy of mixing polymer segment

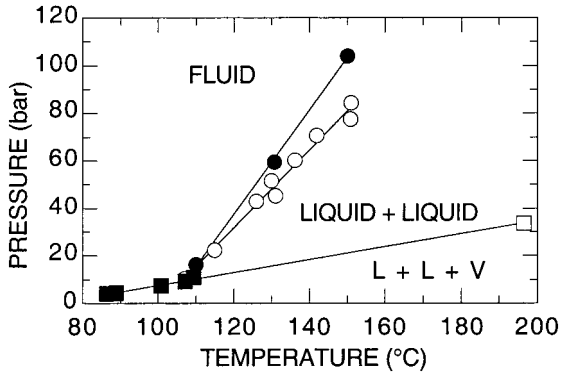

Figure 2. Comparison of the phase behavior of ∼5.0 wt % *h*-PEB-10 in pentane (open circles) and pentane-d_{12} (closed circles). Bubble points (closed squares) are determined experimentally, and the critical point of pentane (open square) is obtained from the literature.[63]

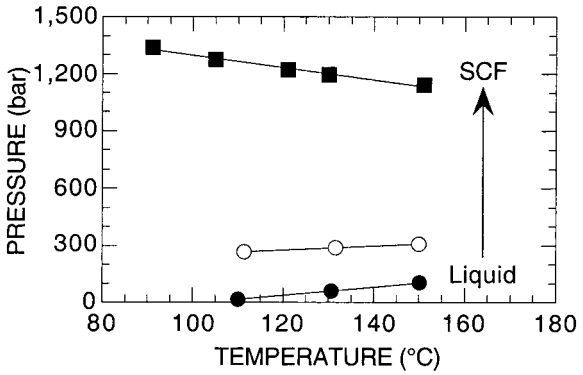

Figure 3. Comparison of the phase behavior of ∼5.0 wt % *h*-PEB-10 in pentane-d_{12} (closed cirlces) and in pentane-d_{12} + 23 wt % ethane (open circles) and the phase behavior of 2.4 wt % *d*-PEB-2 in ethane (closed squares).

(*i*)−solvent (*j*) pairs, ω, given by

$$\omega = z\left[\Gamma_{ij}(r,T) - \frac{1}{2}(\Gamma_{ij}(r,T) + \Gamma_{ij}(r,T))\right] \qquad (1)$$

where z is the coordination number or the number of solvent−segment pairs. Rabinowich[46] shows that the magnitude of dispersion interactions decreases when a deuterium is substituted for hydrogen since the shorter C−D bond length compared to a C−H bond reduces the segment volume and the segment polarizability. In addition, Bates and co-workers[47−49] also show that isotopic labeling causes nonideal behavior for mixtures of high molecular weight polymers.

Figure 3 shows the cloud-point curves for *h*-PEB-10 in pentane-d_{12} and in a mixture of pentane-d_{12} + 23 wt % ethane and for *d*-PEB-2 in pure ethane. The LCST and the upper critical solution temperature (UCST) curves merge when 23 wt % ethane is added to the *h*-PEB-10/pentane-d_{12} mixture, and the composite UCST−LCST curve is located at ∼200 bar higher pressures than the *h*-PEB-10/pentane-d_{12} curve. With pure ethane, the cloud-point pressures are in excess of 1000 bar at temperatures from 90 to 150 °C. The locations of the curves shown in Figure 3 are more directly related to the difference in the solvent quality of supercritical ethane relative to liquid pentane rather than to the modest differences in the molecular weight, degree of chain branching, or polymer concentration in solution.[32] The macroscopic phase behavior demonstrates that supercritical ethane is a very weak solvent

for *h*-PEB-10 relative to liquid pentane. More detailed information on solvent quality is obtained by probing the microstructure of the solution with SANS measurements at pressures near and very far from the phase boundary of the polymer−SCF solvent and polymer−liquid solvent systems.

Small-Angle Neutron Scattering. Intramolecular and intermolecular properties of the polymer in solution defined by R_g and ξ, respectively, are determined by SANS utilizing the high-concentration isotopic labeling technique.[17,50,51] The coherent scattered intensity of an incompressible solution, $I(q)$, is decomposed into a contribution from single chain scattering, $I_s(q)$, and total scattering, $I_t(q)$, according to

$$I(q) = I_s(q) + I_t(q) \tag{2}$$

$$I(q) = Nz^2KS_s(q) + Nz^2LS_t(q) \tag{3}$$

where $S_s(q)$ and $S_t(q)$ are the structure factors of the single chain and total scattering, N is the total number density of polymer molecules, and z is the degree of polymerization. The two contrast parameters K and L are

$$K = (b_h - b_d)^2 x_h x_d \tag{4}$$

$$L = \left(b_h x_h + b_d x_d - \left(\frac{v_p}{v_s}\right) b_s\right)^2 \tag{5}$$

where b_h and b_d are the scattering lengths of hydrogenated and deuterated polymer units, x_h and x_d are the mole fractions of hydrogenated and deuterated chains such that $x_d + x_h = 1$, and $(v_p/v_s)b_s$ is the scattering length of the solvent normalized by the ratio of specific volumes of polymer units (v_p in cm^3/monomer) to solvent molecules (v_s in cm^3/molecule). To determine independently single and total chain scattering, two molar ratios of protonated to deuterated chains are used at an overall polymer concentration equal to the experimentally determined mixture critical concentration. The scattering lengths of the elements[38] are used to determine $b_{h-PEB-10}$, 0.20×10^{-12} cm; $b_{d-PEB-10}$, 1.68×10^{-12} cm; $b_{pentane-d}$, 11.33×10^{-12} cm; and b_{ethane}, 0.91×10^{-12} cm.

To account for the effect of density on the scattering intensities, the densities of the polymer−solvent mixtures, pure ethane, pure pentane-d_{12}, and the pentane-d_{12} + 23 wt % ethane mixture are measured as described elsewhere.[52] Figure 4 shows solution densities at 130 °C that are very close to the densities of the pure and mixed solvents. Although the density of the *d*-PEB-2-ethane solution does not change significantly at the experimental conditions investigated here, the incoherent background of pure ethane at the same conditions is a function of density. Therefore, the *d*-PEB-2-ethane scattering intensities are corrected for compressibility effects by subtracting the density-dependent, incoherent background scattering.

For (*h* or *d*)-PEB-10 dissolved in pentane-d_{12} and pentane-d_{12} + 23 wt % ethane, incoherent backgrounds obtained at high q are insensitive to pressure (density) when operating close to the phase boundary and only slightly sensitive to pressure when operating at high pressures far removed from the phase boundary. The lack of sensitivity is not surprising since both the copolymer and the solvent are very incompressible. The

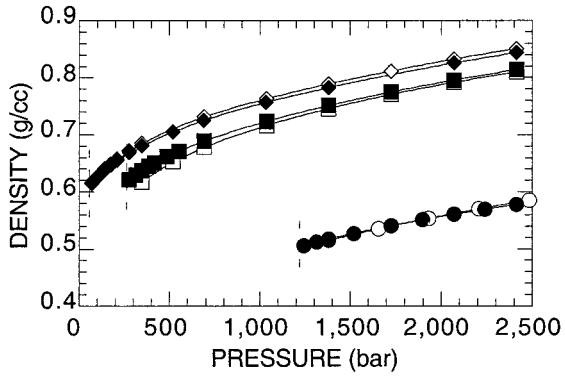

Figure 4. Densities as a function of pressure for ~5.0 wt % *h*-PEB-10 in pentane-d_{12} (closed diamonds), in pentane-d_{12} + 23 wt % ethane (closed squares), and in 2.4 wt % *d*-PEB-2 in ethane (closed circles) and the corresponding pure solvents and the solvent mixture (open symbols) at 130 °C.[52] The dashed lines indicate the location of each solution's cloud-point pressure.

absolute, coherent, total scattering intensities, $I_t(q)$, exhibit a weak dependence on pressure at q greater than ~0.03 Å^{-1}. When the effect of solution density is accounted for in parameters Nz^2 and (v_p/v_s) in eq 3, $S_t(q)$ collapses to a single curve at high q, independent of pressure, and approaches zero in the limit of infinite q. The pressure dependence of the volume of *d*-PEB-2 and PEB-10 polymer segments, v_p, is estimated using the Tait equation[53] with linear and branched PE parameters, respectively.

Total scattering intensities are obtained directly for solutions with x_h equal to one, which forces K to be equal to zero as given in eq 4. The intermolecular correlation length, $\xi(P,T)$, is determined from a fit of the Ornstein−Zernike (OZ) equation to the total chain scattering

$$S_t(q) = \frac{S(0)}{1 + q^2\xi^2} \tag{6}$$

with $S(0)$ as an adjustable parameter. To check for uncertainties in the incoherent backgrounds at high q values, $\xi(P,T)$ is also determined from a fit of the OZ equation to the total scattering intensities, $I_t(q)$, using $I(0)$ and a finite baseline as adjustable parameters. Values of $\xi(P,T)$ obtained by both techniques are virtually identical and agree within the experimental error of ±10% over the entire pressure range investigated. Figure 5 shows the total scattering and resulting OZ fits over the low q range for 4.6 wt % *h*-PEB-10 in pentane-d_{12}. Similar results are obtained for 2.2 wt % *d*-PEB-2 in ethane at 130 and 150 °C and for 4.5 wt % *h*-PEB-10 in pentane-d_{12} + 23 wt % ethane at 130 °C, respectively. The values of $\xi(P,T)$ for each system are listed in Table 1.

A direct measurement of single chain scattering, $S_s(q)$, can be obtained from the scattering of a solution with x_h and x_d chosen so that the contrast variation parameter L equals zero. $S_s(q)$ can also be obtained by subtracting the solution scattering obtained with x_h equal to one from solution scattering with a nonzero value of x_h for a fixed total polymer concentration.[17−20] The *d*-PEB-10 chains used in the present study are only partially deuterated, which means it is not possible to obtain x_h and x_d values that force L to zero. The experimental dilemma in this instance is that a higher amount of *d*-PEB-10 relative to *h*-PEB-10 causes a significant decrease in the signal-to-noise ratio. There-

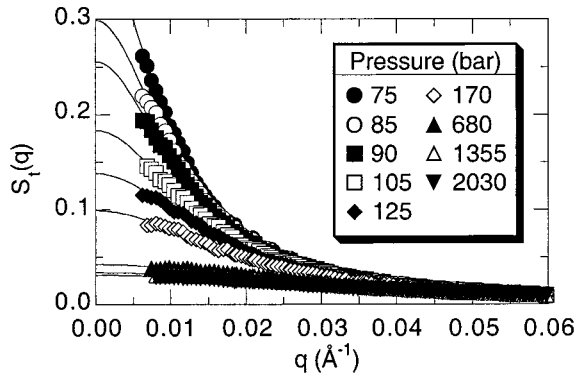

Figure 5. Effect of pressure on the total chain scattering, $S_t(q)$, for 4.6 wt % *h*-PEB-10 in pentane-d_{12} at 130 °C. The smooth curves are fits of the Ornstein−Zernike equation to the data.

Table 1. Correlation Length, $\xi(P,T)$, Values Obtained from the Ornstein−Zernike Equation

	correlation length, ξ (Å)			
press. (bar)	PEB-2 in ethane (130 °C)	PEB-2 in ethane (150 °C)	PEB-10 in pentane (130 °C)	PEB-10 in pentane + ethane (130 °C)
75			104	
85			90	
90			83	
105			71	
125			60	
170			51	
340				116
360				84
375				76
410				66
510				48
680			31	40
1175		139		
1240	135	123		
1355			26	30
1380	107	98		
1520	90	83		
1725	82	73		
2030			25	28
2070	70	67		

fore, to maximize contrast between polymer chains with an efficient signal-to-noise ratio, a value of x_h equal to 0.5 is used with the mixtures of PEB in pure pentane-d_{12} and in the pentane-d_{12} + 23 wt % ethane mixture.

For the SANS studies reported here, *h*-PEB-2 of corresponding M_W was not available for labeling experiments with *d*-PEB-2 in ethane, and the contrast between the partially deuterated *d*-PEB-10 and protonated ethane is too low to obtain acceptable scattering intensities relative to the incoherent background of ethane. Therefore, single-chain scattering for *d*-PEB-2 in ethane is extracted from the total scattering intensities analyzed with the Zimm equation for an arbitrary concentration:[54,55]

$$K'c\left[\frac{d\Sigma}{d\Omega}(q)\right]^{-1} = \frac{1}{M_W S_s(q)} + 2A_2(c)c \qquad (7)$$

where c is the concentration of polymer in solution, K' is the contrast variation parameter, and $A_2(c)$ is the apparent second osmotic virial coefficient, which is concentration dependent. From a Zimm plot of $[(d\Sigma/d\Omega)(q)]^{-1}$ versus q^2, $A_2(c)$ as a function of pressure is determined by fitting the scattering data in the limit as q goes to zero. The values of $A_2(c)$ are then used to correct the scattered intensities for intermolecular interference to obtain an estimate for $S_s(q)$. Intermolecular interference is expected to be sensitive to the amount of polymer chain overlap in solution, which depends on the intermolecular distance, r, between polymer molecules as given by the following estimate:[16]

$$r = \left[\frac{(4\pi c N_A)}{3M_W}\right]^{-1/3} \qquad (8)$$

where N_A is Avogadro's number. When r is equal to R_g, c is equal to the overlap concentration, c^*. Since the polymer concentration increases as the pressure increases, the intermolecular distance between chains also varies from 178 to 172 Å for 2.2 wt % *d*-PEB-2 in ethane, from 148 to 134 Å for 4.6 wt % *h*-PEB-10 in pentane-d_{12}, and from 143 to 133 Å for 4.5 wt % *h*-PEB-10 in pentane-d_{12} + 23 wt % ethane. Over the same pressure ranges, the polymer volume fraction, $\phi_p \sim c_p v_p$, only changes from $0.011 \le \phi_p \le 0.012$ for *d*-PEB-2 in ethane, from $0.029 \le \phi_p \le 0.035$ for *h*-PEB-10 in pentane-d_{12}, and from $0.032 \le \phi_p \le 0.040$ for *h*-PEB-10 in pentane-d_{12} + 23 wt % ethane. Given that $R_{g-\theta,melt}$ is 185 Å for *d*-PEB-2,[26,56,57] and c^* denotes the crossover from the dilute to semidilute concentration regime, the *d*-PEB-2/ethane system is probed at experimental conditions near the onset of coil overlap where chains do not interpenetrate strongly. Hence, intermolecular interference between polymer chains should not have a significant affect on intramolecular dimensions determined with the Zimm equation as described previously. However, since $R_{g-\theta,melt}$ is 205 Å for *h*-PEB-10,[26,56,57] the PEB-10/pentane-d_{12} and PEB-10/pentane-d_{12} + 23 wt % ethane solutions are predominantly in the semidilute concentration regime where the isotopic labeling technique is the more rigorous method for obtaining chain dimensions. A continuation study is in progress with fully deuterated PEB-10 in ethane using the high-concentration isotopic labeling method to confirm the ethane results reported here.

Once the single chain scattering is obtained, R_g at each pressure is determined from a fit of the Debye equation in the low-q scattering range of the data

$$S_s(q) = \frac{2}{q^4 R_g^4}[\exp(-q^2 R_g^2) + q^2 R_g^2 - 1] \qquad (9)$$

Figure 6 shows $S_s(q)$ for PEB-10 in pentane-d_{12} at 130 °C with the corresponding fits of the Debye equation. The inset in Figure 6 shows the log $S_s(q)$ versus q, which indicates good agreement of the SANS data and the Debye equation over the low q range investigated. Similar trends in $S_s(q)$ are observed for all of the other solutions. The R_g values obtained for each system as a function of pressure are listed in Table 2. The R_g values for the *d*-PEB-2−ethane system are corrected for molecular weight polydispersity according to $R^2_{g,w} = R^2_{g,z}[(1+u)/(1+2u)]$ where u is equal to the quantity $[M_W/M_N - 1]$ and M_W/M_N equals 1.09. Corrections for the PEB-10 data are negligible since M_W/M_N is equal to 1.01. R_g values determined from the above methods have an estimated error of ±10−15%.

Discussion

Intramolecular correlations as defined by R_g do not deviate significantly from the unperturbed melt values

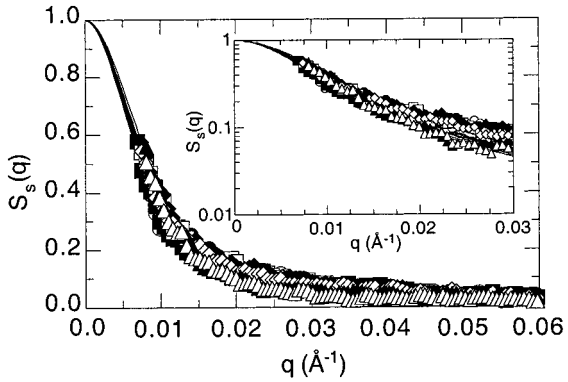

Figure 6. Effect of pressure on single chain scattering, $S_s(q)$, for ~5.0 wt % PEB-10 in pentane-d_{12} at 130 °C and pressures of 75 (closed circles), 85 (open circles), 90 (closed squares), 105 (open squares), 125 (closed diamonds), 170 (open diamonds), 680 (closed triangles), and 1355 bar (open triangles). The smooth curve are fits of the Debye equation, and the inset shows the variation of log $S_s(q)$ over the low q range.

Table 2. Radius of Gyration, R_g, Values Obtained from the Debye Equation

	radius of gyration, R_g (Å)			
press. (bar)	PEB-2 in ethane (130 °C)	PEB-2 in ethane (150 °C)	PEB-10 in pentane (130 °C)	PEB-10 in pentane + ethane (130 °C)
75			198	
85			216	
90			211	
105			194	
125			186	
170			195	
360				197
375				192
410				186
510				221
680			203	229
1175		188		
1240	175	195		
1355			208	
1380	188	185		
1520	184	186		
1725	196	188		
2030				226
2070	191	190		

as the critical point of the solution is approached over the entire pressure range investigated. Figure 7 compares the values of R_g as the critical point is approached isothermally for *d*-PEB-2 in ethane at 130 and 150 °C. The R_g values obtained at each pressure are in excellent agreement with the unperturbed θ-melt value of 185 Å for polyethylene obtained from the power law relationship $R_{g-\theta,melt} \sim 0.45 M_W^{0.5}$.[56,57] The trend observed in R_g is similar to the trends reported for polystyrene in liquid cyclohexane and in liquid acetone.[17−19] Evidently, the PEB chains experience an environment where a modest amount of chain overlap in these near-semidilute solutions causes a screening effect, which induces the chains to mimic meltlike behavior. The PEB/ethane density does not change significantly over the pressure ranges investigated and does not impact intramolecular correlations. A better indication of the solvent strength as a function of pressure is provided by the intermolecular correlation length, which dramatically increases near the critical boundary and begins to approach the magnitude of R_g at pressures near the critical point. The behavior of ξ as a function of distance from the critical point is also shown in Figure 7 for *d*-PEB-2 in ethane. The closest approach to the critical point is ~50 bar

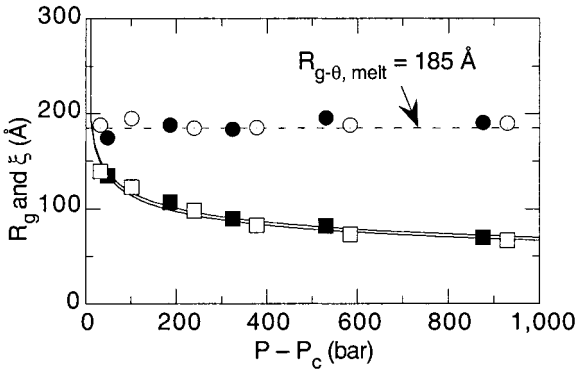

Figure 7. Changes in R_g (circles) and ξ (squares) for 2.2 wt % *d*-PEB-2 in ethane at 130 (closed symbols) and 150 °C (open symbols) as a function of pressure distance to the critical point. The solid curves are power law fits of the data.

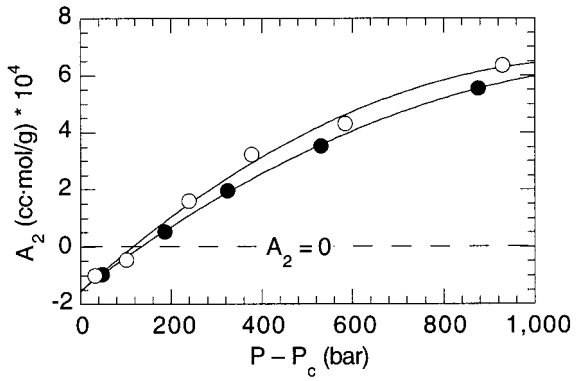

Figure 8. Variation in the second osmotic virial coeffecient, $A_2(c)$, as a function of pressure distance to the critical point for 2.2 wt % *d*-PEB-2 in ethane at 130 (closed circles) and 150 °C (open circles).

while the furthest distance from the critical point is ~1000 bar. As the temperature is increased from 130 to 150 °C, ξ decreases slightly although the trend in the variation in ξ with respect to $P - P_c$ is virtually identical at these two temperatures.

For the *d*-PEB-2/ethane system there are two ways to use the SANS data to locate the θ-pressure, P_θ, which is the demarcation between poor and good solvent quality.[20,58] One way is to extract $A_2(c)$ as a function of pressure from the Zimm analysis applied in the low q range, near qR_g equal to one, and to identify P_θ as the pressure where $A_2(c)$ equals zero, as seen in Figure 8. For the *d*-PEB-2−ethane system, P_θ is ~1330 and ~1260 bar at 130 and 150 °C, respectively. The other way to locate P_θ is from a plot of ξ versus P and the relationship[16,59]

$$\xi_\theta \sim \frac{R_{g,\theta}}{\sqrt{3}} \tag{10}$$

assuming that scattering data are obtained in the low q region. Melnichenko and co-workers[17−20] use this second method to obtain both T_θ and P_θ for a number of different semidilute polymer−liquid solutions. For *d*-PEB-2, $R_{g-\theta}$ is 185 Å, ξ_θ is therefore 107 Å, and P_θ is ~1350 and ~1270 bar at 130 and 150 °C, respectively, which are very close to the values found from the Zimm analysis. It is interesting to note that ethane converts from a θ to a poor solvent at pressures within 155 and 130 bar of the critical point, at 130 and 150 °C, respectively. The trend observed for $A_2(c)$ versus pres-

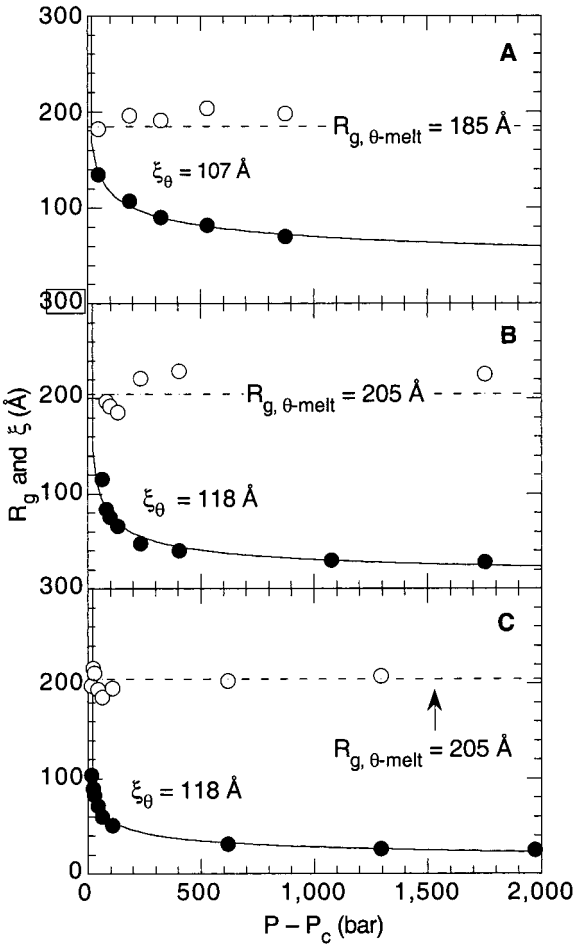

Figure 9. Changes in R_g (open circles) and ξ (closed circles) for (A) *d*-PEB-2 in ethane, (B) PEB-10 in pentane-d_{12} + 23 wt % ethane, and (C) PEB-10 in pentane-d_{12} at 130 °C as a function of pressure distance to the critical point. The solid curves are power law fits of the data.

sure in Figure 8 indicates that solvent quality slowly increases as pressure is increased above the θ-point. It is important to recognize that eq 10 only provides an estimate of the demarcation between θ and poor solvent regimes within the limits of the experimental data. The trend in $A_2(c)$ as a function of pressure for the PEB/ethane mixtures is similar to that observed for poly(isobutylene) in 2-methylbutane and polystyrene in 2-butanone obtained by Gaeckle and Patterson using high-pressure static light scattering.[60] Gaeckle and Patterson suggest that $A_2(c)$ should increase with pressure for solutions in which the free volume contribution to the conformational entropy of mixing dominates solution miscibility when intermolecular interactions between polymer segments and solvent molecules are closely matched.

Figure 9 shows that R_g and ξ exhibit similar behavior for PEB-10 in pentane-d_{12} and in pentane-d_{12} + 23 wt % ethane as compared to the behavior observed with *d*-PEB-2 in ethane. For the PEB-10 solutions, R_g is similar to the unperturbed value of 205 Å found from $R_{g-\theta,\mathrm{melt}} \sim 0.42M_W^{0.5}$.[26] The trends in R_g and ξ shown in Figure 9 appear to be universal in the case of liquid and SCF solvents since they have been observed for a variety of semidilute polymer solutions involving liquids,[17−19] supercritical CO_2,[20] supercritical ethane, and a supercritical pentane + ethane mixed solvent. However, a closer examination of the intermolecular correlation

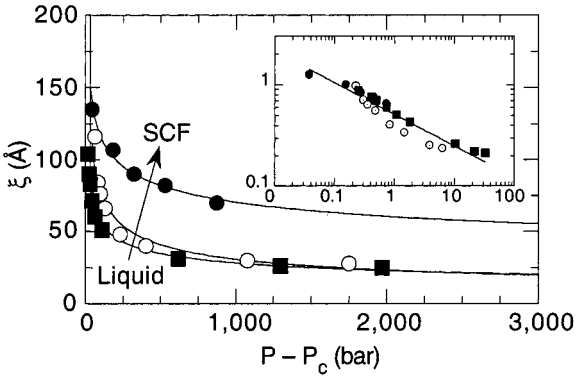

Figure 10. Variation of the correlation length, ξ, on approach to the critical point at 130 °C for *d*-PEB-2 in ethane (closed circles), PEB-10 in pentane-d_{12} + 23 wt % ethane (open circles), and PEB-10 in pentane-d_{12} (closed squares). The solid curves are power law fits of the data. The inset shows a log−log plot of reduced correlation length ξ/ξ_θ versus reduced pressure, $P_r = (P - P_c)/P_c$, with the corresponding power law, $\xi \sim \xi_\theta P_r^{-\upsilon}$, fit to all data with the scaling exponent, υ, equal to ∼0.31.

length shows that there is a dramatic difference in solvent quality between a liquid and a supercritical fluid. Figure 10 shows ξ as a function of the pressure distance to the critical pressure for the three PEB/alkane solutions at 130 °C. The correlation length is larger in the SCF solvent than liquid solvent and remains larger at very far pressure distances from the boundary. This difference in magnitude of ξ between each solution shows that the copolymer solution exhibits larger concentration fluctuations at distances hundreds of bar from the boundary in the SCF solvent that are not seen in the liquid solvent. The inset to Figure 10 is a log−log plot of the reduced correlation length, ξ/ξ_θ, versus the reduced pressure, $P_r = (P - P_c)/P_c$, which shows the three solutions collapse to a single power law curve for this family of poly(olefin)−alkane mixtures. A broader range of polymer systems must be investigated before definitive statements can be made about this interesting behavior.

It is important to note that the *d*-PEB-2/ethane mixture critical concentration is lower than the PEB-10/pentane-d_{12} and PEB-10/pentane-d_{12} + 23 wt % ethane mixture critical concentrations, which results in a slightly lower polymer volume fraction. For a good solvent, the static correlation length for a semidilute solution is expected to increase with decreasing volume fraction according to the relationship[15,61,62]

$$\xi \sim \phi^{-0.75} \tag{11}$$

where ϕ is the polymer volume fraction. Using eq 11 to correct the *d*-PEB-2/ethane ξ values at high pressure accounts for approximately 80% of the difference in ξ between the *d*-PEB-2/ethane and PEB-10/pentane-d_{12} mixtures. It is not apparent that eq 11 should be applied here since ethane does not appear to exhibit good quality solvent behavior as compared to pentane at the high pressures studied and since the *d*-PEB-2/ethane mixture critical concentration is near the dilute regime according to eq 8. In addition, the relationship in eq 11 has only been experimentally proven for a limited number of polymers in incompressible liquid solvents.[16,61,62] Corrections to ξ are not considered in the interpretation of the scattering data presented here; continuation SANS studies are in progress to elucidate the behavior of ξ as a function of pressure, temperature, and polymer con-

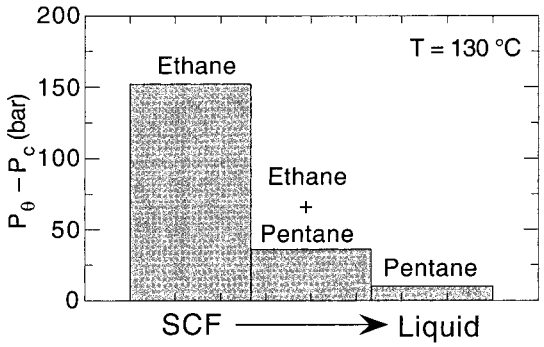

Figure 11. Comparison of poor solvent quality for supercritical ethane, pentane + 23 wt % ethane, and liquid pentane.

centration for polymer−SCF solutions. It is interesting to note the behavior shown in the inset of Figure 10 does not occur if ξ is corrected for the effect of polymer volume fraction.

The difference in ξ for supercritical ethane and liquid pentane as a function of pressure indicates that ethane is weaker solvent than pentane when compared at equivalent distances in pressure to their respective phase boundaries. Similar conclusions are reached if ξ is plotted versus the relative density difference to the critical point or if the scattering at zero angle is plotted versus the relative pressure distance to the critical point. Since the scattering at zero angle, which is directly proportional to the osmotic compressibility,[55] is much larger for ethane than pentane, these data suggest that supercritical ethane is a weak solvent as reflected by the large concentration fluctuations occurring at 1000 bar from the phase boundary. On approach to the phase boundary, $1/S_t(0)$ goes to zero as expected and predicts a critical pressure for each solution within ±20 bar of the experimental observed values obtained from macroscopic phase behavior measurements. The difference in solvent quality between supercritical ethane, pentane plus ethane, and liquid pentane is clearly seen in Figure 11 which compares the magnitudes the poor solvent quality regime defined as the pressure range between the θ and critical points. The values of P_θ are determined from eq 10 and a plot of ξ versus pressure. The poor solvent quality regime extends to 155 bar in ethane, 35 bar in pentane-d_{12} + 23 wt % ethane, and 10 bar in liquid pentane-d_{12}. Figures 10 and 11 suggest the transition from good to θ to poor solvent quality is sharp in liquid pentane whereas the transition in supercritical ethane is less pronounced since intermolecular correlations never reach the values found in liquid pentane, even at 2000 bar. These scattering results are surprising since it strongly suggests that operating in a clear, single-phase region does not ensure that the polymer is uniformly dispersed in the SCF solvent. A more detailed investigation of polymers in liquid versus supercritical fluid solvents is currently being conducted to confirm results presented here and to probe more complex solution behavior than that exhibited by these model nonpolar poly(olefin)−alkane mixtures.

Acknowledgment. The authors acknowledge the National Science Foundation (NSF) for partial support of this project under Grants CTS-9729720 and GER-9454136. Special acknowledgment is given to Pamela Wright and Dr. Lewis Fetters at Exxon Research and Engineering Company for providing high-quality PEB copolymers without which it would not have been possible to perform the isotopic labeling experiments. The authors acknowledge the support of the National Institute of Standards and Technology (NIST), U.S. Department of Commerce, in providing facilities used in this work. This material is based upon activities supported by NSF under Agreement DMR-9423101. In addition, the authors thank Dr. Steven Kline at the NIST Center for Neutron Research for help with the collection and reduction of the SANS data and Tom Kermis and Shawn Conway at JHU for assistance with SANS experiments. The authors are especially indebted to Mike Franckowiac and Walt Krug, master instrument makers at Johns Hopkins University, for assistance with the design of the high-pressure view and scattering cells and for machining the scattering cell.

References and Notes

(1) McHugh, M. A.; Krukonis, V. J. *Supercritical Fluid Extraction: Principles and Practice*, 2nd ed.; Butterworth: Stoneham, MA, 1994.
(2) Berens, A. R.; Huvard, G. S. In *Supercritical Fluid Science and Technology;* ACS Symposium Series 406; Johnston, K. P., Penninger, J. M. L., Eds.; American Chemical Society: Washington, DC, 1989.
(3) Gallagher, P. M.; Coffey, M. P.; Krukonis, V. J.; Klasutis, N. In *Supercritical Fluid Science and Technology;* ACS Symposium Series 406; Johnston, K. P., Penninger, J. M. L., Eds.; American Chemical Society: Washington, DC, 1989.
(4) Johnston, K. P. In *Supercritical Fluid Science and Technology;* ACS Symposium Series 406; Johnston, K. P., Penninger, J. M. L., Eds.; American Chemical Society: Washington, DC, 1989.
(5) McNally, M. E. P.; Deardorff, C. M.; Fahmy, T. M. In *Supercritical Fluid Technology;* ACS Symposium Series 488; Bright, F. V., McNally, M. E. P., Eds.; American Chemical Society: Washington, DC, 1992.
(6) Garrabos, Y.; Leneindre, B.; Subra, P.; Cansell, F.; Pommier, C. *Ann. Chim. Sci. Mater.* **1992**, *17*, 55.
(7) DeSimone, J. M.; Maury, E. E.; Menceloglu, Y. Z.; McClain, J. B.; Romack, T. J.; Combes, J. R. *Science* **1994**, *265*, 356.
(8) Canelas, D. A.; Betts, D. E.; DeSimone, J. M. *Macromolecules* **1996**, *29*, 2818.
(9) Cooper, A. I.; Hems, W. P.; Holmes, B. H. *Macromol. Rapid Commun.* **1998**, *19*, 353.
(10) Poliakoff, M.; Darr, J. A. *Chem. Rev.* **1999**, *99*, 495.
(11) Hasch, B. M.; McHugh, M. A. *J. Polym. Sci., Part B: Polym. Phys. Ed.* **1995**, *33*, 715.
(12) Hasch, B. M.; Lee, S.-H.; McHugh, M. A. *J. Appl. Polym. Sci.* **1996**, *59*, 1107.
(13) Lee, S.-H.; Hasch, B. M.; McHugh, M. A. *Fluid Phase Equilib.* **1996**, *117*, 61.
(14) Kirby, C. F.; McHugh, M. A. *Chem. Rev.* **1999**, *99*, 565.
(15) De Gennes, P.-G. *Scaling Concepts in Polymer Physics*; Cornell University Press: Ithaca, NY, 1979.
(16) Fujita, H. *Polymer Solutions*; Elsevier Science Publishers B. V.: Amsterdam, 1990.
(17) Melnichenko, Y. B.; Wignall, G. D. *Phys. Rev. Lett.* **1997**, *78*, 686.
(18) Melnichenko, Y. B.; Anisimov, M. A.; Povodyrev, A. A.; Wignall, G. D.; J. V.; S.; Van Hook, W. A. *Phys. Rev. Lett.* **1997**, *79*, 5266.
(19) Melnichenko, Y. B.; Wignall, G. D.; Van Hook, W. A.; Szydlowski, J.; Wilczura, H.; Rebelo, L. P. *Macromolecules* **1998**, *31*, 8436.
(20) Melnichenko, Y. R.; Kiran, E.; Wignall, G. D.; Heath, K. D.; Salaniwal, S.; Cochran, H. D.; Stamm, M. *Macromolecules* **1999**, *32*, 5344.
(21) Muthukumar, M. *J. Chem. Phys.* **1986**, *85*, 4722.
(22) Raos, G.; Allegra, G. *J. Chem. Phys.* **1996**, *104*, 1626.
(23) Ehrlich, P.; Kurpen, J. J. *J. Polym. Sci., Part A: Polym. Chem. Ed.* **1963**, *1*, 3217.
(24) Ehrlich, P.; Mortimer, G. A. *Adv. Polym. Sci.* **1970**, *7*, 386.
(25) Hasch, B. M.; Meilchen, M. A.; Lee, S.-H.; McHugh, M. A. *J. Polym. Sci., Part B: Polym. Phys. Ed.* **1992**, *30*, 1365.
(26) Fetters, L. J.; Graessley, W. W.; Krishnamoorti, R.; Lohse, D. J. *Macromolecules* **1997**, *30*, 4973.

(27) Balsara, N. P.; Fetters, L. J.; Hadjichristidis, N.; Lohse, D. J.; Han, C. C.; Graessley, W. W.; Krishnamamoorti, R. *Macromolecules* **1992**, *25*, 6137.
(28) Krigas, T. M.; Carella, J. M.; Struglinski, M. J.; Crist, B.; Graessley, W. W. *J. Polym. Sci., Part B: Polym. Phys. Ed.* **1985**, *23*, 509.
(29) Rachapudy, H.; Smith, G. G.; Raju, V. R.; Graessley, W. W. *J. Polym. Sci., Part B: Polym. Phys. Ed.* **1979**, *17*, 1211.
(30) Mertdogan, C. A.; Byun, H.-S.; McHugh, M. A.; Tuminello, W. H. *Macromolecules* **1996**, *29*, 6548.
(31) Meilchen, M. A.; Hasch, B. M.; McHugh, M. A. *Macromolecules* **1991**, *24*, 4874.
(32) Kirby, C. F.; McHugh, M. A. *Rev. Sci. Instrum.* **1997**, *68*, 3150.
(33) Lentz, H. *Rev. Sci. Instrum.* **1969**, *40*, 371.
(34) Glinka, C. J.; Barker, J. G.; Hammouda, B.; Krueger, S.; Moyer, J. J.; Orts, W. J. *J. Appl. Crystallogr.* **1998**, *31*, 430.
(35) Dubner, W. S.; Schultz, J. M.; Wignall, G. D. *J. Appl. Crystallogr.* **1990**, *23*, 469.
(36) Maconnachie, A. *Polymer* **1984**, *25*, 1068.
(37) Hayashi, H.; Flory, P. J.; Wignall, G. D. *Macromolecules* **1983**, *16*, 1328.
(38) Sears, V. F. *Neutron News* **1992**, *3*, 26.
(39) Vennemann, N.; Lechner, M. D.; Oberthur, R. C. *Polymer* **1987**, *28*, 1738.
(40) Hamada, F.; Fujisawa, K.; Nakajima, A. *Polymer* **1973**, *4*, 316.
(41) Kiran, E.; Zhuang, W. *Polymer* **1992**, *33*, 5259.
(42) Kiran, E.; Zhuang, W.; Sen, Y. L. *J. Appl. Polym. Sci.* **1993**, *47*, 895.
(43) Xiang, Y.; Kiran, E. *J. Appl. Polym. Sci.* **1994**, *53*, 1179.
(44) Kiran, E.; Zhuang, W. In *Supercritical Fluids, Extraction and Pollution Prevention*; American Chemical Society: Washington, DC, 1997.
(45) Zeman, L.; Patterson, D. *J. Phys. Chem.* **1972**, *76*, 1214.
(46) Rabinovich, I. B. *Russ. Chem. Rev.* **1962**, *31*, 51.
(47) Bates, F. S.; Wignall, G. D.; Koehler, W. C. *Phys. Rev. Lett.* **1985**, *55*, 2425.
(48) Bates, F. S.; Wignall, G. D. *Phys. Rev. Lett.* **1986**, *57*, 1429.
(49) Bates, F. S.; Fetters, L. J.; Wignall, G. D. *Macromolecules* **1988**, *21*, 1086.
(50) King, J. S.; Boyer, W.; Wignall, G. D.; Ullman, R. *Macromolecules* **1985**, *18*, 709.
(51) Akcasu, A. Z.; Summerfield, G. C.; Jahshan, S. N.; Han, C. C.; Kim, C. Y.; Yu, H. *J. Polym. Sci., Part B: Polym. Phys. Ed.* **1980**, *18*, 863.
(52) Byun, H. S.; DiNoia, T. P.; McHugh, M. A. *J. Chem. Eng. Data*, in press.
(53) Rodgers, P. A. *J. Appl. Polym. Sci.* **1993**, *48*, 1061.
(54) Benoit, H.; Benmouna, M. *Polymer* **1984**, *25*, 1059.
(55) Higgins, J. S.; Benoit, H. C. *Polymers and Neutron Scattering*; Oxford University Press: New York, 1994.
(56) Schelten, J.; Ballard, D. G. H.; Wignall, G. D.; Longman, G.; Schmatz, W. *Polymer* **1976**, *17*, 751.
(57) Schelten, J.; Wignall, G. D.; Ballard, D. G. H. *Polymer* **1977**, *18*, 1111.
(58) Kiran, E.; Sen, Y. L. In *Supercritical Fluid Engineeing Science;* ACS Symposium Series 514; Kiran, E., Brenneke, J. F., Eds.; American Chemical Society: Washington, DC, 1993.
(59) des Cloizeaux, J.; Jannink, G. *Polymers in Solution: Their Modelling and Structure*; Oxford University Press: Oxford, 1990.
(60) Gaeckle, D.; Patterson, D. *Macromolecules* **1972**, *5*, 136.
(61) Chatterjee, A. P.; Schweizer, K. S. *Macromolecules* **1998**, *31*, 2353.
(62) Tao, H.; Huang, C.; Lodge, T. P. *Macromolecules* **1999**, *32*, 1212.
(63) Reid, R. C.; Prausnitz, J. M.; Poling, B. E. *The Properties of Gases and Liquids*, 4th ed.; McGraw-Hill: New York, 1987.

MA000240Z